# Towards Pre-Clinical Validation of LBM-EP for the Planning and Guidance of Ventricular Tachycardia Ablation

Tommaso Mansi[1], Roy Beinart[2], Oliver Zettinig[1,3], Saikiran Rapaka[1], Bogdan Georgescu[1], Ali Kamen[1], M. Muz Zviman[2], Daniel A. Herzka[4], Henry R. Halperin[3], and Dorin Comaniciu[1]

[1] Imaging and Computer Vision, Siemens Corporation, Corporate Technology, Princeton, NJ, USA
[2] Medicine, Cardiology, Johns Hopkins School of Medicine, Baltimore, MD, USA
[3] Computer Aided Medical Procedures, Technische Universität München, Germany
[4] Biomedical Engineering, Johns Hopkins University, Baltimore, MD, USA
[5] Medicine, Cardiology, Johns Hopkins University, Baltimore, MD, USA

**Abstract.** In this manuscript, a framework for the pre-clinical validation of LBM-EP, a fast cardiac electrophysiology model, is presented. The overarching objective is to assess whether the model is able to predict ventricular tachycardia (VT) induction given the lead location and the pacing frequency protocol. First, the random-walk algorithm is used to interactively segment the heart ventricles from delayed-enhancement magnetic resonance images (DE-MRI). Scar and border zone are delineated using image thresholding. Then, a detailed anatomical model is estimated, comprising fiber architecture and spatial distribution of action potential duration. That information is rasterized to a Cartesian grid, and the cardiac potentials are computed using a parallel implementation of LBM-EP. A preliminary evaluation of the framework was performed on one swine data, for which four different pacing protocols were tested. Each of the protocols were mimicked by computing seven seconds of heart beat. Model predictions in terms of VT induction were compared with what was observed in the animal. Moreover, our parallel implementation on graphics processing units enabled a total computation time of about two minutes at an isotropic grid resolution of $0.8\,mm$, thus allowing, for the first time, interactive VT testing.

## 1 Introduction

Ventricular tachycardia (VT) and ventricular fibrillation are among the most life-threatening cardiac events, causing the majority of the 200,000 yearly sudden deaths. When medication is not sufficient to control them, radio-frequency ablation constitutes an efficient and cost-effective therapy. However, ablation in the setting of healed myocardial infarction has only 58% initial success rate and 71% eventual success rate following repeated procedures [1]. Reasons for these low numbers are: 1) the reentrant pathways to treat are complex and their origination point is challenging to map; 2) ablation is performed point-wise; and

3) registration errors between electrophysiological mapping and anatomy make ablation planning and guidance inaccurate [4]. These limitations not only limit the success of the procedure but also significantly prolong the duration of the intervention and increase the risks of chamber perforation and bleeding. There is therefore a need for new approaches to assist VT ablation therapy prior and during the intervention to improve outcomes.

To tackle this challenge, computational models of cardiac electrophysiology (EP) are being investigated. In [10, 11], preoperative magnetic resonance images (MRI) were employed to generate a model of patient's heart anatomy. Cardiac electrophysiology was then computed using a phenomenological model of action potential [7], with patient-specific parameters estimated from intraoperative endocardial mapping at sinus rhythm [10]. The authors then virtually stimulated the myocardium close to the scar to induce VT. However, in both studies, the results were not validated against clinical observations. In a recent pre-clinical study [8], the authors investigated whether an isotropic EP model, with generic parameters (i.e. non subject-specific), was able to predict VT induction. One protocol and different lead positions were virtually tested on eight pigs, showing promising predictions of VT induction compared to the observed inducibiliy. However, that study did not tackle the question of whether the model was able to predict induction if a specific lead location and protocol was given. Comprehensive validation on clinical setups is therefore still missing.

As a first step towards this aim, we propose a framework for the pre-clinical validation of a fast EP model, LBM-EP [9] in terms of VT planning. In particular, our approach enables to investigate whether LBM-EP can predict VT induction for a specific pacing protocol and lead position. Combining advanced image analysis methods and the LBM-EP model (Sec. 2), our approach allows the fast and streamlined computation of EP for any pacing protocol, interactively. Sec. 3 reports the results of four different pacing protocols in one swine and compare the predicted inducibility with what was observed in that animal. Sec. 4 concludes the manuscript.

## 2 Material and Methods

### 2.1 Pre-Clinical Protocol

**Animal Model** One swine was used in this study. Under general anesthesia, the midleft anterior descending coronary artery was occluded between the first and second diagonal branch for 120 minutes using a $2.7\,Fr$ balloon angioplasty catheter via a femoral artery, to create a myocardial infarction (MI). Sixteen weeks after MI induction, the swine underwent *in-vivo* MRI and two days after the MRI, an EP study was done to determine inducibility of sustained VT.

**Electrophysiological Evaluation** Detailed left ventricular (LV) mapping during sinus rhythm was performed with a multi-electrode 2-$mm$-tip catheter ($6\,Fr$) with $2, 6, 2$-$mm$ inter-electrode spacing (Dynamic XT, Bard Electrophysiology, Lowell) to construct a 3D voltage map using an electro-anatomic mapping system (NavX, St. Jude Medical). Peak-to-peak bipolar amplitudes were displayed

color coded and recorded, with electrograms $\leq 1.5\,mV$ defined as low voltage electrograms. The programmed electrical stimulation protocol was conducted to induce VT using a pacing catheter ($6\,Fr$) advanced to the right and then left ventricular chambers through a femoral vein. The stimulation protocol consisted of three decreasing extra-stimuli at two different drive cycle lengths.

**MRI Protocol** Imaging took place on a 3.0T system with a 32-channel cardiac phased array (Achieva, Philips Medical Systems, Best, The Netherlands). Global cardiac function was measured using 2D breath-hold balanced steady-state free precession ($1.25 \times 1.25 \times 5.0\,mm^3$). For visualization of the border zone and scar, a custom 3D delayed contrast enhancement (DE-MRI) sequence (ECG-gated, respiratory navigator gated, phase-sensitive inversion recovery spoiled gradient echo [6]) with the following imaging parameters was used: 60 slices with 1.00x1.25x3.0 $mm^3$ in-plane resolution reconstructed to $0.75 \times 0.75 \times 1.5\,mm^3$, TR/TE $5.6/2.7\,ms$, 18° flip angle, acquired ≈ 25-35 min post intravenous administration of $0.2\,mmol/kg$ Magnevist (Berlex/Schering AG, Berlin, Germany).

### 2.2 Model of Cardiac Anatomy

We then created the anatomical model from the DE-MRI. An interactive method was employed based on the random-walk algorithm to segment the bi-ventricular myocardium [5]. The resulting masks were fused to form a closed surface of the biventricular myocardium (Fig. 1, left panel). The atria were not considered in this study. Next, the myocardium domain was mapped onto a Cartesian grid and represented as a level-set. Scar and border zone regions were segmented by using image thresholding, and mapped to the Cartesian domain. To cope with tissue anisotropy, a model of fiber architecture was calculated by following a rule-based approach [9]. Below the basal plane, fiber elevation angle varied linearly from the epicardium to the endocardium (from $-60°$ to $+60°$ for the left ventricle (LV), from $-80°$ to $+80°$ for the right ventricle (RV)), which were then geodesically extrapolated up to the valves (Fig. 1, right panel). Finally, a model of the spatial heterogeneity of the action potential distribution (APD) was used [2] by spatially varying the parameter $\tau_{close}$ of the electrophysiology model (see next section). Three types of cells were considered: endocardial ($\tau_{close_{endo}}$), mid-cell ($\tau_{close_{mid}}$) and epicardial ($\tau_{close_{epi}}$), with a slight base-to-apex gradient (base APD was equal to 95% of apex APD, with linear variation throughout the myocardium (Fig. 1, right panel)).

### 2.3 LBM-EP: Lattice-Boltzmann Model of Myocardium Transmembrane Potentials

The LBM-EP method was used to compute cardiac EP in near real-time. LBM-EP solves any mono-domain model by using a Lattice-Boltzmann method [9]. In this work, the trans-membrane potential $v(t) \in [-70\,mV, 30\,mV]$ was calculated

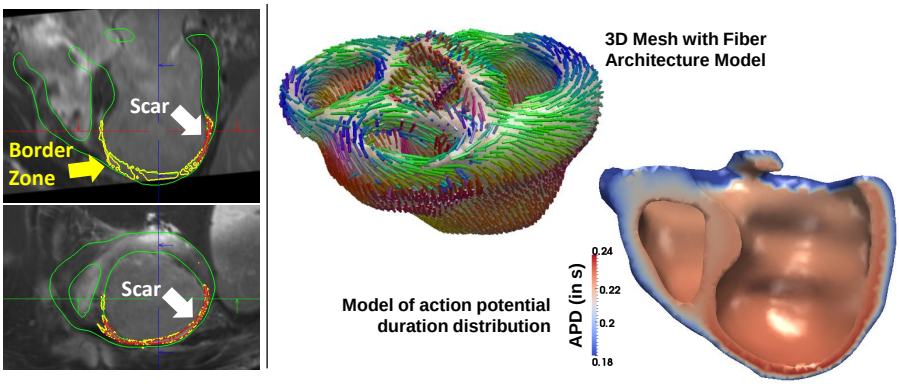


**Fig. 1.** Subject-specific anatomical model. *Left*: Heart segmentation (scar in red). *Right*: Mesh visualization of the anatomical model estimated from the segmentation.

according to the Mitchell-Schaeffer model [7]:

$$\frac{\partial v}{\partial t} = h(t)\frac{v^2(1-v)}{\tau_{in}} - \frac{v}{\tau_{out}} + c\nabla \cdot \mathrm{D}\nabla v + I_{stim}$$
$$\frac{dh}{dt} = \begin{cases} (1-h)/\tau_{open} & \text{if } v < v_{gate} \\ -h/\tau_{close} & \text{otherwise} \end{cases}$$

In the previous equations, $h(t)$ is a gating variable that models the state of the ion channels, $c$ is the tissue diffusivity whose anisotropy is captured by the tensor D and $I_{stim}$ is an additional current (for instance induced by the pacing catheter). The parameters $\tau$ and $v_{gate}$ control the dynamics of the action potential.

The mono-domain equation was solved on a 7-connectivity Cartesian domain (six edges and central position). For higher spatial accuracy, Neumann boundary conditions were enforced by using a level-set representation of the heart anatomy. Stimulation currents were applied through Dirichlet boundary conditions at the position of the pacing lead. Seven different domains were identified on the Cartesian grid: the left and right ventricular septum, used to pace the heart to mimic the His bundle; the left and right endocardia, with fast electrical diffusivity, $c_{LV}$ and $c_{RV}$, to mimic the Purkinje network; the myocardium, with slower diffusivity $c_{Myo}$, the border zone ($c_{bz}$) and the scar, which does not conduct the electrical wave altogether.

We also computed the electrocardiogram resulting from the calculated electrophysiology. The extra-cellular potentials were obtained according to an algebraic equation [3] and mapped to the torso using the boundary element method. Finally, the algorithm was implemented on a graphics processing unit (GPU) for maximal performance.

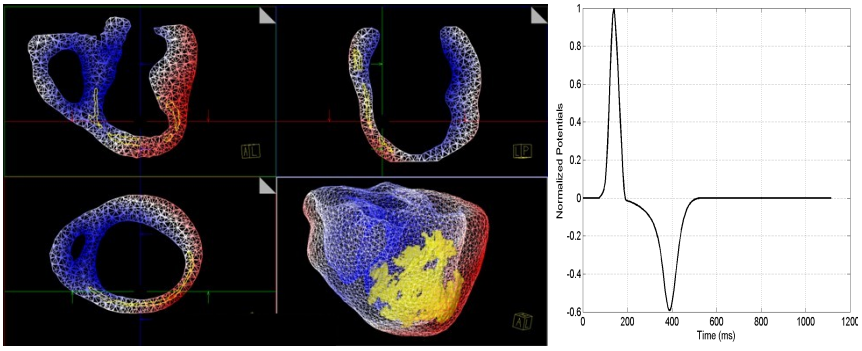


**Fig. 2.** *Left*: Computed depolarization times at sinus rhythm. The scar is highlighted in yellow. *Right*: I-lead ECG resulting from the computed electrophysiology.

### 2.4 Virtual Pacing Protocol

Virtual pacing was performed interactively. The user first chose the protocol to apply in terms of pacing interval. The 3D position of the pacing lead was then placed interactively. Finally, cardiac electrophysiology was computed over the entire pacing session.

## 3 Experiments and Results

### 3.1 Model Personalization

For all experiments, EP was computed on a $0.8 \times 0.8 \times 0.8\,mm^3$ grid. Tissue diffusivity and action potential duration (APD) were manually adjusted to match the measured QRS duration (QRSd = $116\,ms$) and QT interval (QTd = $488\,ms$). Fig. 2 shows the computed depolarization time map and the resulting I-lead electrocardiogram (ECG). After personalization, computed QRSd and QTd matched the measurements: $\text{QRSd}_{comp.} = 115\,ms$ and $\text{QTd}_{comp.} = 450\,ms$ ($c_{LV} = c_{RV} = 2500\,mm^2/s$, $c_{Myo} = 300\,mm^2/s$, $\tau_{close_{endo}} = 180\,ms$, $\tau_{close_{mid}} = 190\,ms$ and $\tau_{close_{epi}} = 140\,ms$). $\tau_{open}$ was globally increased to match trends reported in [10] ($\tau_{open} = 200\,ms$). The nominal values $\tau_{in} = 0.3\,ms$ and $\tau_{out} = 6\,ms$ were used. The diffusivity in the scar was set to $0\,mm^2/s$. Border zone diffusivity was assumed to be half of the healthy tissue, $c_{bz} = 150\,mm^2/s$ while $\tau_{close}$ was increased by $50\,ms$ to mimic the longer APD observed in the healing tissue [8].

### 3.2 Virtual Electrophysiological Evaluation

For all experiments, natural septal pacing occurred at $t = 80\,ms$, then every $1180\,ms$, the measured cycle length. The first S1 stimulus was applied at $t = 1000\,ms$, followed by the subsequent stimulations according to the selected protocol. In total, seven seconds of heart beats were computed. Four pacing protocols were tested (see Fig. 3 for the positions of the lead):

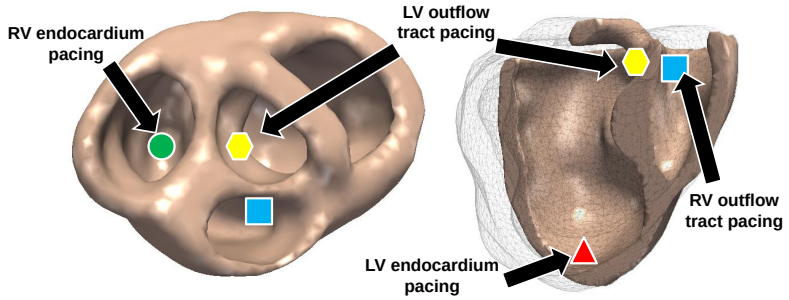


**Fig. 3.** *Left*: Position of the leads for the four VT pacing protocols tested in this study.

**P1: RV endocardium pacing** The lead was placed at the apex of the RV endocardium. Eight stimuli (S1) every 400 $ms$ were applied, followed by the S2 stimulus after 360 $ms$, S3 after 320 $ms$ and S4 after 290 $ms$.

**P2: RV outflow tract pacing** The lead was placed at the RV outflow tract. The same stimulation protocol as for the RV endocardium apex was employed.

**P3: LV endocardium pacing** The lead was placed at the LV endocardium apex, where no scar nor border zone was present. Eight times S1 stimuli were applied every 450 $ms$, then S2 after 310 $ms$, S3 after 250 $ms$ and S4 after 230 $ms$.

**P4: LV outflow tract pacing** The lead was placed at the LV outflow tract. The same stimulation protocol as for the LV endocardium apex was employed.

Fig. 4, left panel reports the computed I-lead ECG traces for the four pacing protocols. For all of them, sustained VT could not be induced. For P1, P2 and P3, the model is in agreement with what was observed experimentally, where no sustained VT could be obtained. For P4 however, three monomorphic VT cycles could be induced in the animal, which eventually degenerated in ventricular fibrillation. From the computed ECGs, one can see that S2, S3 and S4 stimuli fall in some cases in the refractory period of the heart, thus not triggering heart depolarization (S3 for P1, S4 for P2, P3 and P4). Experimentally, this was not the case: all pacing lead to cardiac depolarization. This suggests further personalization is needed, in particular regarding the parameters controlling the APD restitution curve.

### 3.3 Computational Efficiency

On a standard desktop machine (Intel Xeon 8-core @ 2.4 GHz, 4GB RAM, NVIDIA GeForce GTX 580), EP over 1 $s$ was computed in 19.5 $s$, yielding approximatively 2 minutes of computation for a complete VT pacing protocol. To the best of our knowledge, this is the first time interactive virtual VT study could be performed at relatively high resolution. Further speed-up could be achieved

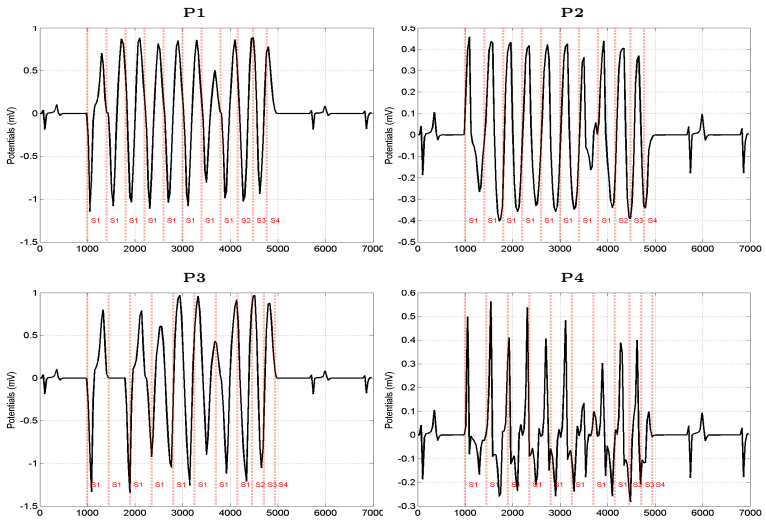


**Fig. 4.** Computed I-lead ECG for the four tested pacing protocols. None of them induced sustained VT after the end of the stimulations. See text for details.

by using lower resolution, at the price of the accuracy (1 $s$ required 3.8 $s$ of computation at 1.5 $mm$ resolution for instance) or by using a more powerful graphics card, LBM-EP being highly scalable both in terms of computational node and number of cores.

## 4 Discussion and Conclusion

This manuscript presented a framework for the animal validation of LBM-EP, a fast computational model of cardiac electrophysiology, in terms of prediction of VT induction and ablation. Our approach couples advanced image analytics for patient-specific anatomical modeling with a GPU-implementation of LBM-EP and a model of ECG. Two minutes are needed to compute 7s of heart beat, which is enough to detect if VT can be induced or not, compared to the 14 hours needed in [8]. Our framework thus enables, for the first time to the best of our knowledge, interactive virtual electrophysiological evaluations. A preliminary evaluation against four pacing protocols in one swine suggested promising results. However, further personalization is required for improved predictions. The next steps consist in comprehensive and quantitative evaluation against ECG signals and invasive endocardial mapping, along with a sensitivity analysis of the model predictions with respect to scar and border zone segmentation accuracy, as well as lead position and S1 starting time.

## References


1. Aliot, E.M., Stevenson, W.G., Almendral-Garrote, J.M., Bogun, F., Calkins, C.H., Delacretaz, E., Della Bella, P., Hindricks, G., Jaïs, P., Josephson, M.E., et al.: Ehra/hrs expert consensus on catheter ablation of ventricular arrhythmias developed in a partnership with the european heart rhythm association (ehra), a registered branch of the european society of cardiology (esc), and the heart rhythm society (hrs); in collaboration with the american college of cardiology (acc) and the american heart association (aha). Europace 11(6), 771–817 (2009)
2. Boulakia, M., Cazeau, S., Fernández, M.A., Gerbeau, J.F., Zemzemi, N.: Mathematical modeling of electrocardiograms: a numerical study. Annals of biomedical engineering 38(3), 1071–1097 (2010)
3. Chhay, M., Coudière, Y., Turpault, R.: How to compute the extracellular potential in electrocardiology from an extended monodomain model. Research Report RR-7916, INRIA (Mar 2012)
4. De Bakker, J., Van Capelle, F., Janse, M., Wilde, A., Coronel, R., Becker, A., Dingemans, K., Van Hemel, N., Hauer, R.: Reentry as a cause of ventricular tachycardia in patients with chronic ischemic heart disease: electrophysiologic and anatomic correlation. Circulation 77(3), 589–606 (1988)
5. Grady, L.: Random walks for image segmentation. Pattern Analysis and Machine Intelligence, IEEE Transactions on 28(11), 1768–1783 (2006)
6. Lee, S.L., Schär, M., Kozerke, S., Harouni, A.A., Sena-Weltin, V., Zviman, M.M., Halperin, H., McVeigh, E.R., Herzka, D.A.: Independent respiratory navigators for improved 3d psir imaging of myocardial infarctions. Journal of Cardiovascular Magnetic Resonance 13(Suppl 1), P18 (2011)
7. Mitchell, C., Schaeffer, D.: A two-current model for the dynamics of cardiac membrane. Bulletin of mathematical biology 65(5), 767–793 (2003)
8. Ng, J., Jacobson, J.T., Ng, J.K., Gordon, D., Lee, D.C., Carr, J.C., Goldberger, J.J.: Virtual electrophysiological study in a 3-dimensional cardiac magnetic resonance imaging model of porcine myocardial infarction. Journal of the American College of Cardiology 60(5), 423–430 (2012)
9. Rapaka, S., Mansi, T., Georgescu, B., Pop, M., Wright, G., Kamen, A., Comaniciu, D.: LBM-EP: Lattice-boltzmann method for fast cardiac electrophysiology simulation from 3d images. In: Proc. MICCAI 2012, LNCS, vol. 7511. Springer (2012)
10. Relan, J., Chinchapatnam, P., Sermesant, M., Rhode, K., Ginks, M., Delingette, H., Rinaldi, C.A., Razavi, R., Ayache, N.: Coupled personalization of cardiac electrophysiology models for prediction of ischaemic ventricular tachycardia. J. R. Soc. Interface Focus 1(3), 396–407 (2011)
11. Talbot, H., Marchesseau, S., Duriez, C., Sermesant, M., Cotin, S., Delingette, H.: Towards an interactive electromechanical model of the heart. Interface Focus 3(2) (2013)